

IMECE2003-41442

## AC ELECTROKINETICS FOR MICROFLUIDIC IMMUNOSENSORS

M. Sigurdson, C. Meinhart, D. Wang, X. Liu  
Mechanical Engineering Department  
University of California  
Santa Barbara, CA 93106

J.J. Feng, S. Krishnamoorthy, S. Sundaram  
CFD Research Corporation  
Huntsville, AL, USA 35806

### ABSTRACT

A technique is proposed to enhance microfluidic immuno-sensors, specifically, sensors in which a ligand immobilized within a microchannel binds analyte flowing through the channel for the purpose of detection of that analyte. These sensors can be limited in both response time and sensitivity by the diffusion of analyte to the sensing surface. The sensitivity and response of these heterogeneous immunoassays may be improved by using AC electrokinetically-driven microscale fluid motion to enhance antigen motion towards immobilized ligands. Specifically, electrothermal effects can produce swirling flow patterns that carry sample past the binding surface. Numerical simulations of antigen in a microchannel flow subjected to the electrothermal effect suggest that 14 V rms applied to electrodes strategically placed opposite a narrow binding region can increase binding in the first few minutes by a factor of five. Optimization of the electrode geometry and placement can render this technique useful for a large variety of microfluidic sensors.

### INTRODUCTION

Immunoassays, which rely on specific antigen-antibody binding for identification of proteins in a sample, have applications in both clinical laboratories for medical diagnostics and treatment monitoring, and in research laboratories for highly multiplexed testing, such as for biomarker identification. In these cases, throughput is a key consideration. One factor limiting throughput is diffusion of analyte to the reporter. An incubation step of minutes to hours allows diffusion-limited binding to reach detectable levels. These tests are usually performed at centralized labs where high throughput is achieved through robotics and highly parallel assays. However, if the assay could be moved from the centralized lab to the point of care – realizing immunoassay-based diagnostics “on demand” – the test must be faster, as well as smaller, while maintaining high sensitivity.

In response to this need, Microfluidic assays for diagnostics have developed dramatically in recent years, allowing the realization of the lab-on-a-chip concepts for point-of-care diagnosis and high throughput screening for molecular diagnostics. Small length scales permit small sample sizes and shorter assay times; on-chip sample preparation reduces fluid handling steps. Though greatly aided by their small length scales, these assays can still be limited in response by diffusion of the analyte to the immobilized ligand. The AC Electrokinetics Enhancement method addresses the need for faster assays by offering a tool, adaptable to a wide variety of assay configurations, which will reduce the incubation time required to perform a specific test while maintaining its sensitivity.

### NOMENCLATURE

$B$  bound antigen concentration  
 $C$  unbound antigen concentration  
 $C_T$  inlet antigen concentration  
 $D$  antigen diffusivity  
ETF: Electrothermally driven flow  
 $k_a, k_d$  antigen-antibody forward and reverse rate constants  
 $K$  Clausius-Mosotti factor  
 $R_T$  immobilized conjugate antibody concentration  
 $\sigma$  electrical conductivity  
 $\varepsilon$  permittivity

### ELECTROKINETIC PHENOMENA

Electrokinetic phenomena are important at micron length scales, and can be used to manipulate fluid and particle motion in microfluidic devices. Electrokinetics can be broadly classified into DC and AC electrokinetics, as shown in Table 1. DC electrokinetic phenomena include electrophoresis and electroosmosis. Electrophoresis has been widely used in capillary gel electrophoresis for fractionation of DNA, and capillary zone electrophoresis for separation of chemical

Table 1. Classification of AC and DC electrokinetic phenomena

Type of Force	AC Electrokinetics	DC Electrokinetics
Body Force on Fluid	Electrothermal	
Surface Force on Fluid	AC Electroosmosis	Electroosmosis
Force on Suspended Particles	Dielectrophoresis	Electrophoresis

species (Thormann, 01). DC Electroosmosis is widely used for sample injection and transport in microchannels in commercial systems manufactured by companies such as Aclara and Caliper (Chien, 02; Bousse, 00). AC electrokinetics, on the other hand, has received limited attention in the microfluidics community, compared to its DC counterpart. A primary advantage of AC electrokinetics is that the alternating fields significantly reduce electrolysis at the electrodes. In addition, the characteristic voltages are typically of order 10's of volts, which are typically much smaller than DC electrokinetics. AC electrokinetics refers to induced particle and/or fluid motion resulting from externally applied AC electric fields. AC electrokinetics can be classified into three broad areas: dielectrophoresis (DEP), electrothermal forces and AC electroosmosis (Ramos *et al.*, 1998).

Dielectrophoresis is a force arising from differences in polarizability between the particle and the fluid medium in the presence of a non-uniform electric field. DEP has been used to separate blood cells and to capture DNA molecules (Miles *et al.*, 1999; Wang *et al.* 1998; Washizu *et al.*, 1995; & Yang *et al.*, 1999; Gascoyne, 2002, provides an overview). However, since the force scales with the cube of particle radius, it is most effective in manipulating particles of order one micron or larger, and not smaller (<100nm) antigen.

AC Electroosmosis arises when the tangential component of the electric field interacts with a double layer along a surface. It becomes less important with increasing electric field frequency. For example, in an aqueous saline solution with an electrical conductivity of  $\sigma = 2 \times 10^{-3}$  S/m, it is predicted that AC electroosmosis is not important above 100 kHz (Ramos, 02).

Transport enhancement for small proteins may be most successful through electrothermally driven flow (ETF). A non-uniform electric field produces uneven Joule heating of the fluid, which gives rise to nonuniformities in conductivity and permittivity. These interact with the electric field to generate flow. Characteristic swirling flow patterns can be used to circulate suspended molecules past the binding region, thereby providing more binding opportunity for the suspended molecules.

## NUMERICAL SIMULATION OF ETF

The finite element package CFD-ACE+ (CFD Research Corp, Huntsville, AL) was used for preliminary predictions of electrothermally-induced flow and subsequent enhanced binding in the cavity. First, the quasi-static potential field for two long electrodes along the cavity wall is calculated (Fig. 1a). The non-uniform electric field gives rise to non-uniform temperature fields through Joule heating. Ignoring unsteady effects and convection, and balancing thermal diffusion with Joule heating yields

$$k\nabla^2 T + \sigma E^2 = 0, \quad (1)$$

where  $T$  is temperature and  $E^2$  is the magnitude squared of the electric field, given by  $\vec{E} = -\nabla V$ , where  $k$  and  $\sigma$  are the thermal and electrical conductivity. The temperature field solution is shown in Figure 1b.

Gradients in temperature produce gradients in permittivity and conductivity in the fluid. For water ( $1/\sigma$ ) ( $\partial\sigma/\partial T$ ) = +2% and  $(1/\epsilon)$  ( $\partial\epsilon/\partial T$ ) = -0.4% per degree Kelvin. These variations in electric properties produce gradients in charge density and perturb the electric field. Assuming the perturbed electric field is much smaller than the applied electric field, and that advection of electric charge is small compared to conduction, the time-averaged electrothermal force per unit volume for a non-dispersive fluid can be written as (Ramos *et al.*, 1998)

$$\vec{F}_{ET} = -0.5 \left[ \left( \frac{\nabla\sigma}{\sigma} - \frac{\nabla\epsilon}{\epsilon} \right) \vec{E}_{rms} \frac{\epsilon \vec{E}_{rms}}{1 + (\omega\tau)^2} + 0.5 \left| \vec{E}_{rms} \right|^2 \nabla\epsilon \right] \quad (2)$$

where  $\tau = \epsilon/\sigma$  is the charge relaxation time of the fluid medium and the incremental temperature-dependent changes are

$$\nabla\epsilon = \left( \frac{\partial\epsilon}{\partial T} \right) \nabla T, \quad \nabla\sigma = \left( \frac{\partial\sigma}{\partial T} \right) \nabla T \quad (3)$$

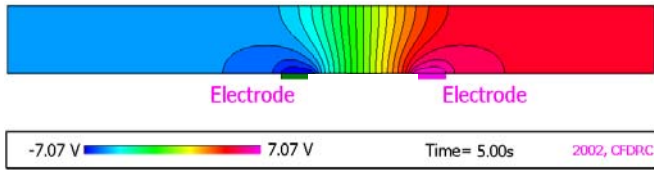
The first term on the right hand side of Eq. (2) is the Coulombic force, and is dominant at low frequencies. The second term is the dielectric force, and is dominant at high frequencies. The crossover frequency scales inversely with the charge relaxation time of the fluid, and typically occurs at around several MHz.

The electrothermal force shown in Eq. (2) is a body force on the fluid. The motion of the fluid can be determined by solving the Stokes' equation for zero Reynolds number fluid flow, such that

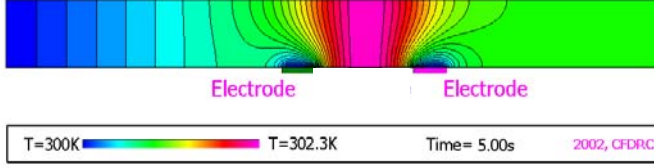
$$0 = -\nabla P + \mu \nabla^2 \vec{u} + \vec{F}_{ET}, \quad (4)$$

where  $\vec{u}$  is the fluid velocity,  $P$  is the pressure in the fluid, and  $\mu$  is the dynamic viscosity of the fluid. Figure 5 shows the resulting velocity field. The velocity of the ETF is of order 300  $\mu\text{m/s}$ , and characterized by a pair of counter rotating vortices. From Fig. 1c, the velocity field shows that the fluid is convected with small eddy motions, which may effectively stir the analyte. If antibodies have been immobilized on the channel wall in a region of increased flow, these eddy motions will transport antigen to the antibody binding region.

(a) Potential field



(b) Temperature field



(c) Velocity Field (Center section only to show detail)

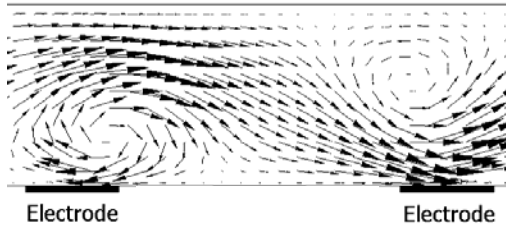


Figure 1. Calculations of electrothermally-driven flow in a 40  $\mu\text{m}$  channel using CFD-ACE+ software. (a) Quasi-static electric potential across two electrodes, (b) non-uniform temperature distribution created by Joule heating, and (c) Electrothermally-driven fluid motion. The mean channel flow is moving from left to right at about a velocity of approximately 100  $\mu\text{m/s}$ . The velocity of the electrothermally-driven flow is of order 300  $\mu\text{m/s}$  and is characterized by a pair of counter rotating vortices. Simulations courtesy of CFDRC.

## EFFECT OF ETF ON BINDING

We now investigate the effect these flow patterns may have on the binding response of an assay in which antibody has been immobilized along a short length of the microchannel wall. The convective scalar equation predicts the suspended concentration  $C(x,y)$  of antigen within the microchannel:

$$\frac{\partial C}{\partial t} + \vec{u} \cdot \nabla C = D \nabla^2 C, \quad (5)$$

where  $\vec{u}$  is the fluid velocity and  $D$  the diffusivity of the antigen. An antigen concentration of  $C_0 = 0.1 \text{ nM}$  is impulsively introduced into the left hand side of the channel. Since the base flow is parabolic, analyte will be transported downstream most rapidly at the channel center. This is shown in Fig. 2a, where the highest concentrations of analyte extend at the center of the channel, and no concentration has yet reached the sensor binding site. When an electric potential is applied to the electrodes, the electrothermally-induced motion transports the analyte close to the upper surface of the channel (Fig. 2b). This suggests that for these flow conditions and electrode configuration, an excellent sensor location is above the first electrode.

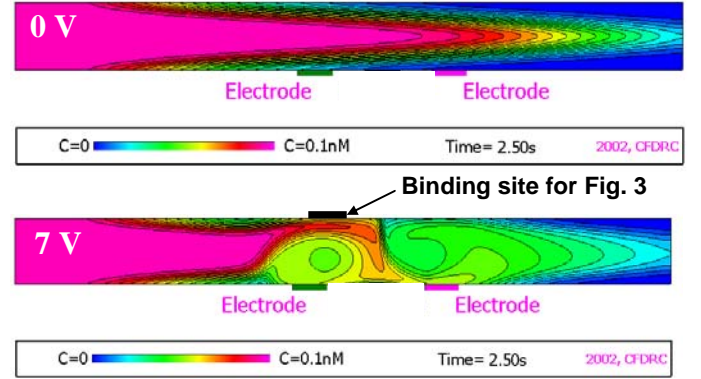


Figure 2. Concentration plots of electrothermally modified channel flow with applied voltages of 0V and 7V. With optimal size and placement of electrodes, the electrothermal eddies can be engineered to span width of the channel, as is the case here, for a 40 micron channel. High concentration gradients and therefore an increase in diffusive flux in the vertical direction near the top channel wall indicate a favorable alternative location for the sensor here.

Following the model given by Myszka *et al.* (98), the rate of association is  $k_a C_w (R_T - B)$ , where  $k_a$  is the association constant,  $R_T - B$  is the available antibody concentration, and  $C_w(x)$  is the suspended concentration of antigen along the wall. The rate of dissociation is  $k_d B$ , where  $k_d$  is the dissociation constant, and  $B$  is the concentration of bound antigen. The time rate of change of antigen bound to the immobilized antibodies is equal to the rate of association minus the rate of dissociation

$$\frac{\partial B}{\partial t} = k_a C_w (R_T - B) - k_d B. \quad (6)$$

The rate of antigen binding to immobilized antigen,  $\partial B / \partial t$ , must be balanced by the diffusive flux of antigen at the binding surface,  $y = 0$ , such that

$$\frac{\partial B}{\partial t} = D \left. \frac{\partial C}{\partial y} \right|_{y=0}. \quad (7)$$

Equations (5), (6) & (7) are solved with an initial antigen concentration  $C_0 = 0.1 \text{ nM}$ , and an immobilized antibody concentration  $R_T = 1.7 \text{ nM cm}$  (i.e. one molecule per 100  $\text{nm}^2$ ). The binding rates for three conditions, 0V, 7V and 14 V root-mean-square voltage, are shown in Fig. 3. The 0V case corresponds to the passive case, which is the result of pure diffusion. This is the standard mode of most immobilized assays. The 7V and 14V curves correspond to the result of electrothermally-driven flow enhancing the transport of antigen to the immobilized antibodies. The curves in Fig. 3 show that a factor of up to 5 (500%) improvement in response is obtained by using AC electrokinetics.

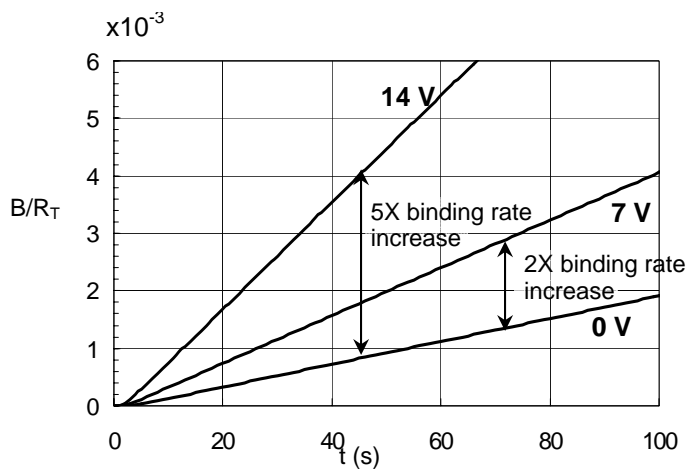


Figure 3: Microchannel enhancement. . Numerical simulation of normalized bound concentration for microchannel assay: with 7V applied rms voltage, the binding rate is about double the non-enhanced binding rate. With 14 Vrms applied, the binding rate jumps to 5 times the non-enhanced rate. These results suggest that electrothermally induced flow can significantly improve immunoassay performance by increasing binding rates. Inlet channel flow rate averages 100  $\mu\text{m/s}$

This technique can also be optimized for microcavity or microarray assays where the sample is not continuously flowing. These simulations yield somewhat better enhancement, as shown in Figure 4. In this case, the binding region is located coplanar with and between the electrodes.

The AC frequency is 100kHz. In this range, the electrothermal velocity is not very sensitive to frequency. Competing effects such as AC electroosmosis and electrode polarization may dominate at lower frequencies; at much higher frequencies, the dielectric component of the electrothermal force (last term in Eq. 2) dominates (Ramos, 02).

Although temperature rises in these simulations are only on the order of a few degrees throughout the channel, and around a degree over the binding area, for the most sensitive assays, it may be desirable to reduce this temperature difference further. Electrodes as well as microchannel walls can be designed by varying geometry and material, to effectively transport heat to or from the microchannel. In this way, temperature can be controlled somewhat independently of electric field. Additionally, since the temperature field can be both predictable and constant after a brief initial transient period, a high sensitivity assay may be able to sustain a larger temperature differential across the binding region if that temperature differential is known and corrected for.

## CONCLUSIONS

By designing a microchannel electrode system that takes advantage of electrothermal effects, cross-stream transport of an antigen and hence binding can be enhanced. Numerical simulations here predict factors of 2~8 improvement; with electrode and heat transfer optimization, an order of magnitude increase in binding rate may be achieved. This enhancement technique can be applicable to a wide variety of assay formats.

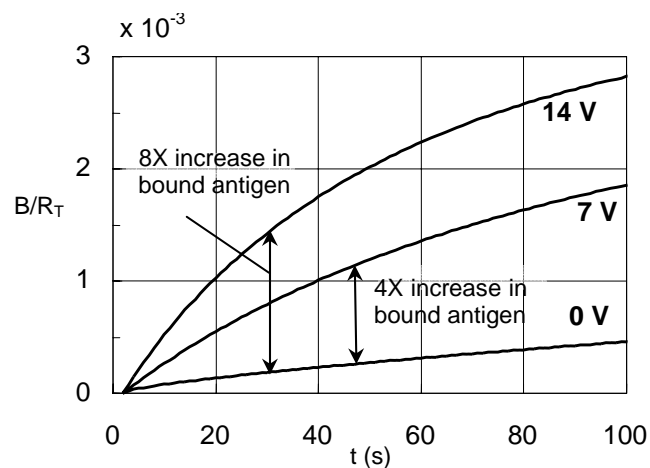


Figure 4: Microcavity enhancement. Numerical simulation of normalized bound concentration for non-flow-through (cavity) assay; non-enhanced (0 V) and enhanced (7V, 14V) transport. The differences in the two curves show an increase in binding rate which yields a factor of 4 higher binding for 7 V and a factor of 8 higher binding after 30 seconds for 14 V applied root-mean square potential. The binding improvement for the 14 V case decreases to around 6 X after 100 seconds: the binding is no longer completely transport-limited.

## ACKNOWLEDGMENTS

This work has been funded by DARPA grants No. 99-110 and 19-00-1-0400 under the BioFlips and SymbioSys programs.

## REFERENCES

- Bousse L. Cohen C. Nikiforov T. Chow A. Kopf-Sill AR. Dubrow R. Parce JW. Electrokinetically controlled microfluidic analysis systems [Review]. *Annual Review of Biophysics & Biomolecular Structure*. 29:155-181, 2000.
- Chien, Ring-Ling et al., Simultaneous hydrodynamic and electrokinetic flow control, *Micro Total Analysis Systems 2002, Volume 1*, 386-388, November, 2002.
- Gascoyne PRC. Vykoukal J. Particle separation by dielectrophoresis [Review]. *Electrophoresis*. 23(13):1973-1983, 2002 Jul.
- Miles, R., P. Belgrader, K. Bettencourt, J. Hamilton, S. Nasarabadi, 1999. Dielectrophoretic manipulation of particles for use in microfluidic devices, *MEMS-Vol. 1, Microelectromechanical Systems (MEMS), Proceedings of the ASME International Mechanical Engineering Congress and Exposition*, Nashville, TN, Nov. 14 – 19.
- Myszka, D.G. 1998. Survey of the 1998 optical biosensor literature. *J Mol. Recognit*. Vol. 12, pp. 390-408.
- Ramos, A., A. Castellanos, A. Gonzales, H. Morgan, N. Green. Manipulation of Bio-Particles in Microelectrode Structures by means of Non-Uniform AC Electric Fields. *Proceedings of ASME International Mechanical Engineering Congress & Exposition* Nov. 17-22, 2002, New Orleans, LA.
- Ramos, A., H. Morgan, N.G. Green and A. Castellanos, 1998. AC electrokinetics: a review of forces in microelectrode structures. *J. Phys. D: Appl. Phys.* 31, 2338–2353.

- Thormann, W., I. Lurie, B. McCord, U. Mareti, B. Cenni, N. Malik. Advances of capillary electrophoresis in clinical and forensic analysis (1999–2000). *Electrophoresis* 2001, 22, 4216-4243.
- Washizu, M., O. Kurosawa, I. Arai, S. Suzuki, N. Shimamoto, 1995 Applications of electrostatic stretch and positioning of DNA, *IEEE Transactions on Industry Applications*, Vol. 32, No. 3, pp. 447-445.
- Yang, J. Huang, Y., Wang, X., Wang, X-B, Becker, F. Gascoyne, P. 1999. Dielectric properties of human leukocyte subpopulations determined by electrorotation as a cell separation criterion. *Biophysical Journal*, Vol. 76, pp. 3307-3314.
- Wang, X-B, Vykoukal, J., Becker, F. & Gascoyne, P. 1998. Separation of polystyrene microbeads using dielectrophoretic/gravitational field-flow-fractionation. *Biophysical Journal*, Vol. 74, pp. 2689-2701.